International Journal of Multimedia and Ubiquitous Engineering
Vol.11, No.6 (2016), pp.119-130
http://dx.doi.org/10.14257/ijmue.2016.11.6.11

# Investigation of Thermal Response Model for Solar Irradiance Absolute Radiometer

Xiaolong Yi[1,2], Wei Fang[1], Yang Luo[1], Xin Ye[1], Dongjun Yang[1] and Yupeng Wang[1*]

[1]*Changchun Institute of Optics, Fine Mechanics and Physics, Chinese Academy of Sciences, Changchun 130033, China*
[2]*University of Chinese Academy of Sciences, Beijing 100049, China*
**corresponding author: wangyp@ciomp.ac.cn;*

***Abstract***

*Solar Irradiance Absolute Radiometer (SIAR) is a cavity-type electrical substitution radiometer for transferring the World Radiance Reference (WRR). In order to shorten the measurement period, and ensure the measurement precision, the cavity temperature response model is experimentally investigated and corrected. The thermodynamic equation of cavity temperature is solved. Based on the analysis of non-equivalent in optical and electrical heating, the cavity temperature response model is corrected to a double exponential form. The simulation result analyzes the origin of the temperature pulse. A new characteristic parameter, named as non-equivalent response time, is proposed and measured. The cavity temperature response characteristic of SIAR is improved by the compensation of the temperature pulse. Comparison experiment results illustrate that the temperature pulse can be compensated by inserting a delay time, and the cavity temperature response model is simplified to a single exponential form. Thus, SIAR with large thermal time constant can adopt shorter measurement period, meanwhile measurement precision is 0.07%. The investigation of non-equivalent response time is important for the radiant calibration of SIAR. This correction method can also be used to optimize the on-orbit calibration method of Total Solar Irradiance Monitor (TSIM).*

***Keywords****: Absolute radiometer; Thermal response model; Non-equivalent; Radiant calibration*

## 1. Introduction

Total Solar Irradiance (TSI) study is necessary to understand different contributions to global climate changes [1-4]. Increasing number of Total Solar Irradiance Radiometers (TSIRs) has conducted long-term high-precision measurement on space platforms since 1978 [5-7]. The amplitude of the variation is 0.1% during an 11-year solar cycle [8]. The Total Solar Irradiance Monitors (TSIMs), developed by Changchun Institute of Optics, Fine Mechanics and Physics (CIOMP) for China Meteorological Administration (CMA), have been operated on the Feng Yun satellites (FY-3A and FY-3B) for long-term TSI measurement [9-10]. TSI measurement data is in good agreement with the measurement data in the same period. TSIM/FY-3C was launched on 2014 [11]. Measurement mode adopts solar-tracking to replace wide-view scanning, in order to improve effective measurement time and measurement accuracy. The tracking accuracy is superior to 0.3° [12].

In order to calibrate different TSIRs, World Meteorological Organization (WMO) established World Radiance Reference (WRR) [13]. WMO conducts International Pyrheliometers Comparison (IPC) every five years. TSIMs' traceability to WRR can be obtained by ground-based radiant calibration. CIOMP commenced the development of absolute radiometers since last century 60's. Solar Irradiance Absolute Radiometer

ISSN: 1975-0080 IJMUE

(SIAR), developed by CIOMP, has attended IPC for three times [14]. The absolute deviation between SIAR-2a and WRR is only 0.00042, and measurement precision is superior to 0.080% [15]. SIAR can be used as transfer detector for calibrating TSIMs.

SIAR is a cavity-type electrical substitution radiometer. The solar irradiance is absorbed by a cavity, resulting in a temperature rise. When the temperature rise is reappeared by an equivalent electrical power, the solar irradiance can be achieved by precisely measuring the equivalent electrical power. Under the heating of optical or electrical power, the cavity temperature response curve conforms to a single exponential form [16]. The $\tau$ is thermal time constant. The time of $10\tau$ is needed to recover equilibrium state. SIAR adopts the method of dynamic forecast compensated electrical power [15]. Measurement process is consisted of radiant observation and electrical calibration. In radiant observation, the radiant power and the compensated electrical power are both provided to the cavity in order to maintain the thermal equilibrium state. According to the single exponential model, the equilibrium temperature can be forecasted by the temperature variation at the initial phase of radiant observation. Then the compensated electrical power is corrected by the forecasted equilibrium temperature, in order to ensure that the total heating powers of radiant observation and electrical calibration are both approximated to 75mW. This method significantly shortens the measurement period because the equilibrium state can be quickly recovered. After several corrections, the total heating powers of radiant observation and electrical calibration are gradually approaching. Therefore, the cavity temperature should be constant during measure process. But practical application finds that there are fixed temperature pulses at the initial phase of radiant observation and electrical calibration. The temperature pulse destroys equilibrium state, and forces SIAR to extend measurement period. The investigation shows that each SIAR has a different temperature pulse.

In order to attend the IPC-XII, the fourth generation of SIAR is improved in both electrical and mechanical design. The characteristic parameter of SIAR mainly contains the thermal time constant, which represents the cavity temperature response speed. The thermal time constant is depended on the heat capacity and heat conductivity. Limited by the manufacturing technology, each SIAR has different thermal time constants. Therefore the optimum measurement periods are different. At present, the measurement period of 90 seconds is generally used in IPC. Due to the impact of the temperature pulse, SIAR with large thermal time constant cannot adopt the measurement period of 90 seconds. Thus, the investigation and compensation of temperature pulse is necessary. In this paper, the cavity temperature response model is corrected according to the investigation of heat conduction structure. A new characteristic parameter, named as non-equivalent response time, is proposed and measured. The temperature pulse is compensated by inserting a delay time. The cavity temperature response curve is significantly optimized. Then the time of recovering equilibrium state is shortened. Thus SIAR with large thermal time constant can adopt small measurement period, meanwhile, the measurement precision is improved.

## 2. Correction of Cavity Temperature Response Model

### 2.1. Detector Structure of SIAR

SIAR is a cavity-type electrical substitution radiometer. The primary cavity and the reference cavity are connected with the heat sink by thermal links as shown in Figure1. When the shutter is open, radiant power is absorbed in primary cavity, resulting in a temperature rise. The thermocouple outputs a voltage, which is entitled as temperature voltage. The sampling code of temperature voltage represents the cavity temperature in practical measurement. The temperature variation of heat sink is compensated by the dual cavity inter-compensating structure [17]. The electrical power is loaded on the primary cavity by an electrical heater. The radiant power is obtained by accurately measuring the equivalent electrical power.

 

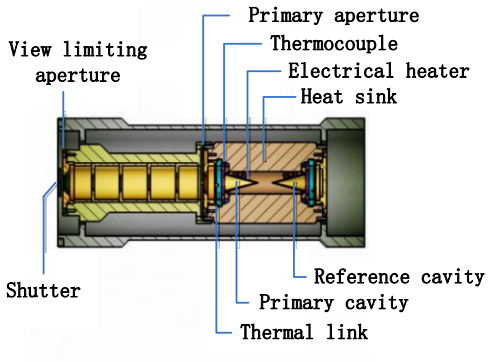


**Figure 1. The Detector Structure of SIAR**

### 2.2 Establishment of Cavity Temperature Response Model

The heat conduction structure of SIAR belongs to the problem of single temperature sensor. According to the centralized parameter method, the primary cavity and heat sink are simplified to mass points [18-19], which have no relationship with spatial coordinates as shown in Figure2. The cavity temperature is $T_C(t)$, and the heat sink temperature is $T_H(t)$.

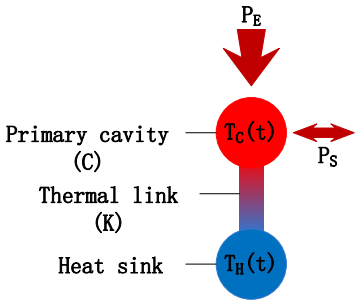


**Figure 2. One Dimensional Heat Conduction Structure**

The thermodynamic equation for cavity temperature is as follows

$$\frac{dT_C(t)}{dt} = \frac{\varphi}{\rho c}, \tag{1}$$

Where $\rho$ is the material density, $c$ is the specific heat, and $\varphi$ is the generating heat of heat source in unit time per unit volume. The $\varphi$ contains three parts: the power transferred from cavity to heat sink ($\varphi_1$); the heating power ($\varphi_2$); the radiant heat between cavity and shutter ($\varphi_3$). They are respectively expressed by

$$\varphi_1 V = -[T_C(t) - T_H(t)] / R, \tag{2}$$

$$\varphi_2 V = P, \tag{3}$$

$$\varphi_3 V = P_S, \tag{4}$$

Where $V$ is the volume of cavity, $R$ is the thermal resistance of thermal link, $P$ is heating power, and $P_S$ is the radiant power between cavity and shutter. Under the heating of electrical power ($P_E$), the thermodynamic equation is obtained by Eq.1 to Eq.4, and depicted by

$$C\frac{dT_C(t)}{dt} = K[T_H(t) - T_C(t)] + P_E + P_S, \tag{5}$$

Where $C=V\rho c$ is the total heat capacity of cavity, $K=1/R$ is the heat conductivity of thermal link. According to the Planck's law, $P_S$ is calculated by

$$P_S = \int_0^{2\pi}\int_0^{\omega_h}(\frac{\sigma\varepsilon T_C^{\ 4}}{\pi} - \frac{\sigma\varepsilon T_S^{\ 4}}{\pi})\cos\theta\sin\theta d\theta d\psi \quad , \tag{6}$$

Where $T_S$ is the shutter temperature, $\sigma$=5.670×10$^{-8}$W/(m$^2$K$^4$) is Stepan Boltzmann constant, $\varepsilon$ is the radiation intensity of shutter and primary cavity, and $\omega_h$ is half view field. The temperature difference between primary cavity and heat sink is expressed by

$$T_d(t) = T_C(t) - T_H(t) \quad . \tag{7}$$

Due to the temperature of heat sink is constant, Eq.5 is derived as

$$C\frac{\mathrm{d}T_d(t)}{\mathrm{d}t} + KT_d(t) = P_E + P_S \quad . \tag{8}$$

When $t$=0, the cavity temperature is $T$. Then Eq.8 can be solved. The transient temperature response model accords with single exponential model, which is expressed by

$$T_d(t) = T_0 + (T - T_0)\ e^{-\frac{t}{\tau}} \quad , \tag{9}$$

Where $\tau=C/K$ is thermal time constant, $T_0$ is equilibrium temperature, and depicted by

$$T_0 = (P_E + P_S)/K \quad . \tag{10}$$

When $t\to\infty$, Eq.9 is rewritten as

$$\lim_{t\to\infty} T_d(t) = \lim_{t\to\infty} T_0(1 + e^{-\frac{t}{\tau}}) = T_0 \quad . \tag{11}$$

Thus when heated by a constant power, cavity temperature response has a single exponential form as shown in Eq.9. Generally, the temperature at the time of 10$\tau$ is used as the equilibrium temperature. The time for recovering equilibrium state is depended on the thermal time constant, which is a characteristic parameter of SIAR.

### 2.3. Correction of Cavity Temperature Response Model

The single exponential model is established on the assumption that the primary cavity and heat sink are both mass points. But the cavity temperature response process is complex in practical heating process. According to the qualitative analysis of heating mode, the cavity temperature response model is corrected.

#### 2.3.1 Cavity Manufacture Technology

The cavity is manufactured by electrical accumulation method with silver material. Electrical heater is covered inside cavity wall as shown in Figure3. The inside surface of cavity is coated with a specular reflecting black paint [20]. The outside of cavity is painted with gold to be used as protective layer. Through multiple reflecting, the 99.96% of radiant power is absorbed by black paint, and transformed to cavity temperature rise. Considering heating mode and surface, radiant and electrical heating is non-equivalent.

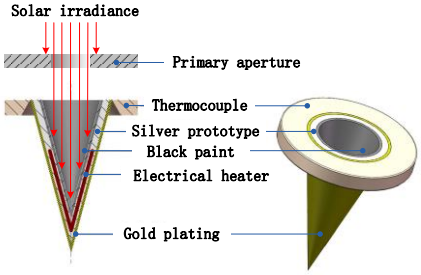


**Figure 3. The Structure of Cavity**

 

### 2.3.2. Non-Equivalent Response Time

The radiant power is transformed by black paint, but the electrical power is transformed by electrical heater. Due to the different heat conduction modes, the radiant and electrical heating have different heat conductivities. $K$ has an inversely-proportional relationship with $\tau$. Thus radiant and electrical heating have different thermal time constants. Under the heating of electrical power, cavity temperature is balanced to $T$ firstly. Then under radiant and electrical heating, the cavity temperature response can be obtained by the linear accumulation of Eq.9, and expressed by

$$T_d(t) = T_{E0} + (T - T_{E0})e^{-\frac{t}{\tau_E}} + T_{O0} + (0 - T_{O0})e^{-\frac{t}{\tau_O}}, \quad (12)$$

Where $\tau_E$ is the thermal time constant of electrical power, $\tau_O$ is the thermal time constant of radiant power, $T_{E0}$ is the equilibrium temperature of electrical power, $T_{O0}$ is the equilibrium temperature of radiant power.

Eq.12 is the double exponential model of cavity temperature response. The difference between thermal time constants is named as non-equivalent response time ($a$), which is expressed as

$$a = \tau_E - \tau_O. \quad (13)$$

Based on LabVIEW, the double exponential model of cavity temperature response is established according to Eq.12. The cavity temperature response is simulated as shown in Figure4. The radiant power and electrical power are constant. The cavity temperature responses are different under diverse non-equivalent response times. Simulation results illustrate that non-equivalent response time leads to the temperature pulse of cavity temperature response. Meanwhile, temperature pulse has a proportional relationship with non-equivalent response time. Thus, the non-equivalent response time is an important characteristic parameter of SIAR. The non-equivalence between radiant and electrical heating is the reason of temperature pulse. The double exponential model is more accurate in practical measurement.

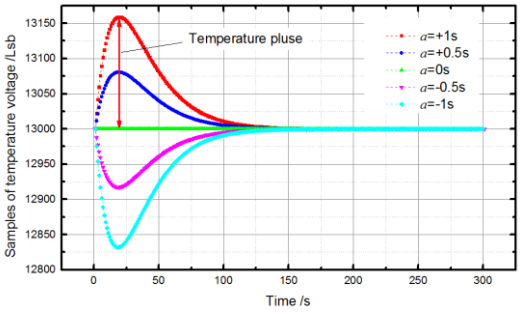


**Figure 4. The Simulation Result of Cavity Temperature Response under Diverse Non-Equivalent Response Times**

## 3. Measurement of Non-Equivalent Response Time

The fourth generation of SIAR is improved in both electrical and mechanical design. Limited by manufacture technology, each SIAR has a different thermal time constant and non-equivalent response time. The thermal time constant and non-equivalent response time are experimentally measured after assembly.

### 3.1. Measurement Process

Radiant source adopts halogen tungsten lamp, which has a power stability superior to 0.1%. In the first place, radiant power ($P_O$) is repeatedly measured by SIAR in order to

obtain the equivalent electrical power ($P_E$). Then the sampling frequency of SIAR is improved from 1Hz to 5Hz. Under radiant power heating, the rise and decline curves of cavity temperature response are respectively measured. Afterwards, under radiant power heating, the rise and decline curves of cavity temperature response are respectively measured. Finally, thermal time constants are obtained by fitting cavity temperature response curves, and non-equivalent response time is calculated.

### 3.2. Measurement Result

SIAR-4A, SIAR-4B, SIAR-4C and SIAR-4D are respectively measured. The first 20 samples of rise and decline curves are shown in Figure5. Both in rise and decline processes, the response speeds of the electrical power are slower than the radiant power. There is a delay value ($t$) between the two cavity temperature response curves. Meanwhile the delay value is identical in the rise and decline processes. Each SIAR has a diverse delay value. The measurement results of thermal time constant, non-equivalent response time and delay value are shown in Table.1. Experiment results illustrate that the non-equivalent response time is the reason of temperature pulse, and corresponds to the delay value of cavity temperature response curves. Thus, the non-equivalent response time is an important characteristic parameter of SIAR.

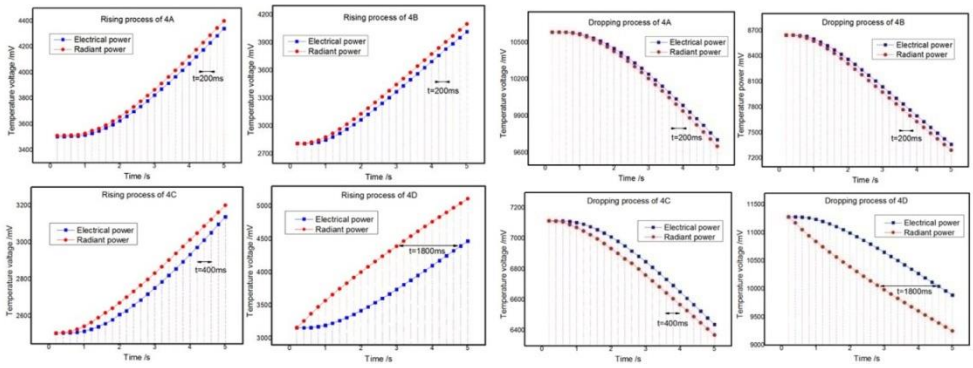


(a) The Rise Process (b) The Decline Process

**Figure 5. The First 20 Samples of Cavity Temperature Response Curves**

**Table 1. Measurement Results of Non-Equivalent Response Time**

| SIAR | Thermal time constant | | Non-equivalent response time | Delay value |
|---|---|---|---|---|
| | $\tau_O$ /s | $\tau_E$ /s | $a$ /s | t /s |
| 4A | 18.54 | 18.60 | 0.08 | 0.2 |
| 4B | 14.17 | 14.24 | 0.07 | 0.2 |
| 4C | 16.09 | 16.54 | 0.45 | 0.4 |
| 4D | 16.54 | 17.23 | 0.69 | 1.8 |

## 4. Measure Method Optimization for SIAR

### 4.1 Principle of dynamic forecast compensated electrical power

Before measurement, the sensitivity ($S$) is calculated by self-test [16]. $S$ represents the relationship between cavity temperature and electrical power. Then under preheating of electrical power ($P_H$), cavity obtains an equilibrium temperature ($T_H$).

Shutter is opened in radiant observation. Radiant power ($P_O$) is absorbed by primary cavity. Meanwhile a compensated electrical power ($P_E$) is loaded on primary cavity in order to maintain thermal equilibrium state. Prof. Bing-xi Yu assumes that cavity temperature response curve accords with single exponential model [15]. Then according to

 

the cavity temperatures (T($t_1$) and T($t_2$)) at the initial phase, the equilibrium temperature ($T_O$) of $P_O$ and $P_E$ can be calculated by

$$T_O = \frac{T(t_2) - e^{(-\frac{t_2 - t_1}{\tau})} T(t_1)}{1 - e^{(-\frac{t_2 - t_1}{\tau})}} . \quad (14)$$

In order to obtain the same equilibrium temperature with $T_H$ in radiant observation, the sum of $P_O$ and $P_E$ should be equal to $P_H$. Thus $P_E$ is corrected by $P_{E1}$, which is calculated by

$$P_{E1} = P_E + (T_H - T_O) \times S . \quad (15)$$

Then under the heating of $P_O$ and $P_{E1}$, the equilibrium temperature of radiant observation is $T_{O1}$.

Shutter is closed in electrical calibration. Cavity is only heated by the electrical power ($P_{E2}$), which is equal to $P_H$

$$P_{E2} = P_H . \quad (16)$$

Then the equilibrium temperature of electrical calibration is $T_{E2}$. Thus $P_O$ is depicted as

$$P_O = P_{E2} - P_{E1} + (T_{O1} - T_{E2}) \times S . \quad (17)$$

In practical measurement, the sum of $P_O$ and $P_{E1}$ is quite approaching to $P_H$ after several correcting. Thus cavity temperature should be constant in measure process. But there are fixed temperature pulses at the initial phases of radiant observation and electrical calibration as shown in Figure6. According to the analysis of Section 2.3, the reason of temperature pulse is that the response speed of SIAR to radiant power is faster than electrical power. Thus under the heating of $P_O$ and $P_{E1}$, the double exponential model of cavity temperature response is more accurate.

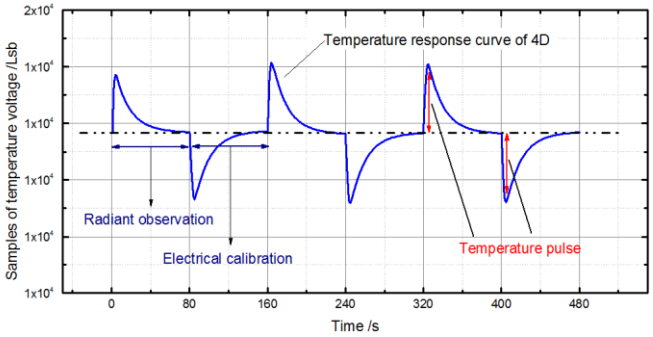


**Figure 6. Temperature Pulses Exist in the Initial Phases of Radiant Observation or Electrical Calibration**

### 4.2 Correction Method Principle

In order to compensate the temperature pulse, the measure process is improved as follows. At the initial phase of radiant observation, the electrical power is reduced first. Then shutter is opened after a period of time, and the radiant power is loaded on the primary cavity. At the initial phase of electrical calibration, the electrical power is increased first. Then shutter is closed after the same period of time. Therefore, a delay time ($t_C$) is inserted into the measure process. The insertion of delay time is equivalent to move the cavity temperature response curve of radiant power to the right. The movement distance is $t_C$. When $t_C$=$t$, cavity temperature response curves are rapidly coinciding as shown in Figure7. Thus, the delay time can compensate the difference of cavity temperature response speed. The temperature pulse can be eliminated. Therefore, the cavity temperature response curve in measure process is corrected.

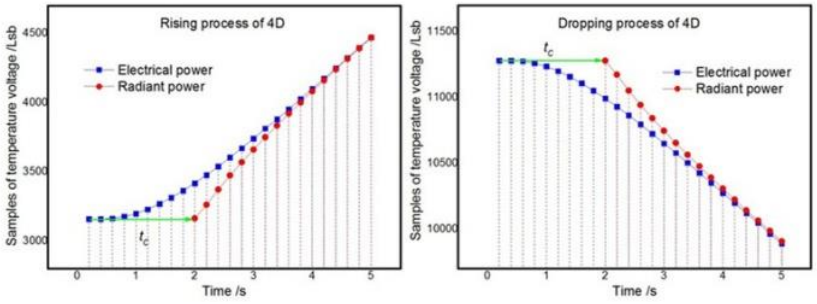


(a) Rise Process (b) Decline Process

**Figure 7. The Compensation of Cavity Temperature Response Speed Difference**

Meanwhile, according to the measurement result of Section 3.2, the delay value corresponds to non-equivalent response time. Thus, the insertion of delay time is also equivalent to increase $\tau_O$. Then Eq.12 is depicted as

$$T_d(t) = T_{E0} + (T - T_{E0})e^{-\frac{t}{\tau_E}} + T_{O0} + (0 - T_{O0})e^{-\frac{t}{\tau_O + a}}. \quad (18)$$

When the non-equivalent response time accords with Eq.13, the double exponential model of cavity temperature response curve is simplified as

$$T_d(t) = T_{E0} + T_{O0} + (T - T_{E0} - T_{O0})e^{-\frac{t}{\tau_O + a}}. \quad (19)$$

Thus, the delay time can compensate non-equivalent response time. The cavity temperature response curve is simplified to the single exponential model. Then, the accuracy of equilibrium temperature forecast is improved.

### 4.3. Comparison Experiments

The measurement result of non-equivalent response time illustrates that SIAR-4D not only has a large thermal time constant ($\tau \approx 17$s), but also has a big non-equivalent response time. When measurement period is set to 90s (measurement periods of radiant observation and electrical calibration are respectively 45s), cavity temperature cannot achieve equilibrium state because of the temperature pulse. Meanwhile, there is a big difference between the equilibrium temperatures of radiant observation and electrical calibration. Therefore, the measurement precision is reduced.

#### 4.3.1. Improvement of Cavity Temperature Response

When the non-equivalent response time is measured, the cavity temperature response can be improved by inserting $t_C$. The measurement period is set to 160s (the measurement periods of radiant observation and electrical calibration are respectively 80s). Then a series of $t_C$ is inserted in the measurement process of SIAR-4D. The radiant power of halogen tungsten lamp is repeatedly measured. A series of cavity temperature response curves are obtained as shown in Figure8. Experiment results illustrate that the temperature pulse is declining along with the increasing of $t_C$. The time of recovering equilibrium state is shortened. When the delay time is equivalent to the delay value, the temperature pulse is the minimum, and the time of recovering equilibrium state is the shortest (only needs 35s). When $t_C$=0s, the time of recovering equilibrium state needs 70s at least. Experiment result illustrates that the delay value is compensated by the delay time. The elimination of temperature pulse shortens the time of recovering equilibrium state. Thus, the SIAR with big thermal time constant also can adopt little measurement period.

 

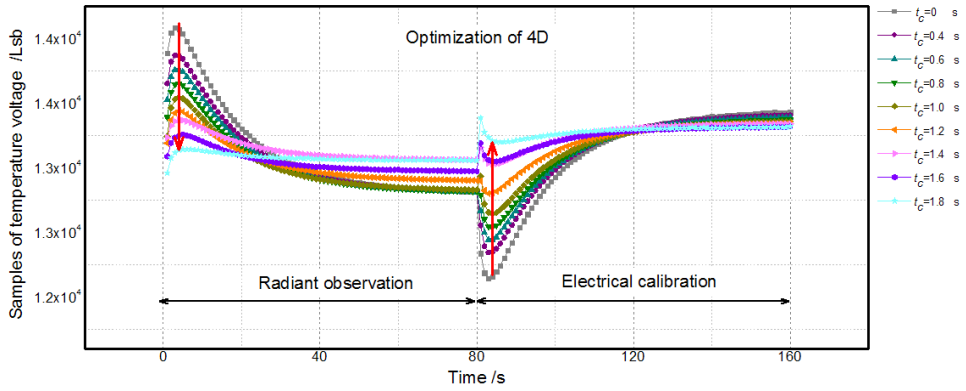


**Figure 8. Measurement Period Optimization of SIAR-4D**

Meanwhile experiment result in Figure8 also illustrates that the difference of equilibrium temperatures is gradually decreasing with increasing the delay time. Therefore, the accuracy of equilibrium temperature forecast is improved.

The measurement period of SIAR-4D is set to 90s, which is generally used in IPC. The measurement periods of radiant observation and electrical calibration are respectively 45s. Then delay time is respectively set to 1.8s or 0s. The radiant power of halogen tungsten lamp is repeatedly measured as shown in Figure9. Experimental result illustrates that measurement accuracy is improved from 0.13% to 0.07%. Because that the insertion of delay time shortens the time of recovering equilibrium state, and the accuracy of equilibrium temperature forecast is improved.

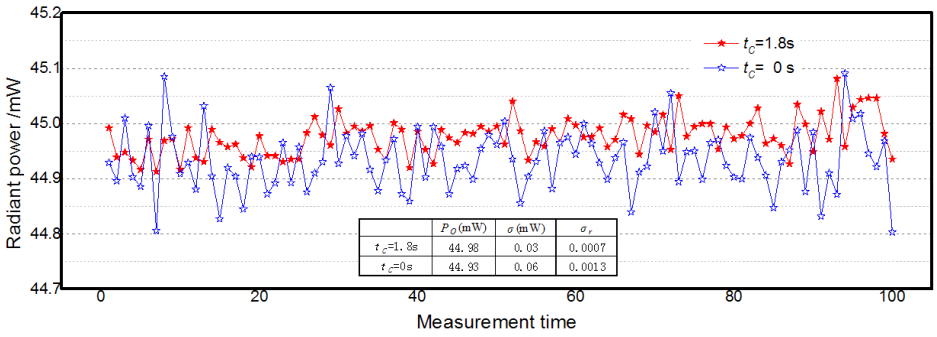


**Figure 9. Measurement Result Comparison**

### 4.3.2. Uncertainty Analysis

The electrical power is obtained by measuring the voltage code of electrical heater. Electrical power is depicted as

$$P_E = \frac{D^2 V_S^{\ 2}}{D_S^{\ 2} R}, \tag{19}$$

Where $V_S$ is the reference voltage of AD, $D_S$ is the code of reference voltage, $R$ is the resistance of electrical heater. According to Eq.17 and Eq.19, the radiant power is expressed as

$$P_O = \frac{(D_2^{\ 2} - D_1^{\ 2}) V_S^{\ 2}}{D_S^{\ 2} R} + \Delta \times S, \tag{20}$$

Where $\Delta = T_{O1} - T_{E1}$ is the difference of equilibrium temperatures, $D_2$ is the sampling code of heat voltage in electrical calibration, $D_1$ is the sampling code of heat voltage in

radiant observation. The absolute uncertainty of SIAR is calculated by

$$u^2 = (\frac{\partial P_O}{\partial D_2})^2 u^2(D_2) + (\frac{\partial P_O}{\partial D_1})^2 u^2(D_1) + (\frac{\partial P_O}{\partial V_S})^2 u^2(V_S) + \frac{\partial P_O}{\partial D_S})^2 u^2(D_S) + (\frac{\partial P_O}{\partial R})^2 u^2(R) + (\frac{\partial P_O}{\partial \Delta})^2 u^2(\Delta) + (\frac{\partial P_O}{\partial S})^2 u^2(S)$$
$$= (\frac{2V_S^2 D_2}{D_S^2 R})^2 u^2(D_2) + (\frac{2V_S^2 D_1}{D_S^2 R})^2 u^2(D_1) + (\frac{2V_S(D_2^2 - D_1^2)}{D_S^2 R})^2 u^2(V_S) + (\frac{2(D_2^2 - D_1^2)V_S^2}{D_S^3 R})^2 u^2(D_S) + (\frac{(D_2^2 - D_1^2)V_S^2}{D_S^2 R^2})^2 u^2(R) + S^2 u^2(\Delta) + \Delta^2 u^2(S) \quad (21)$$

According to the uncertainty components listed in Table.2, the absolute uncertainty ($u$) of SIAR is 0.028mW, and relative uncertainty ($u_r$) is 0.06%. If the confidence factor ($k$) is 2, $2u_r$=0.12%＞0.07%. Thus the optimization of SIAR can shorten measurement period, and can guarantee the measure accuracy.

**Table 2. Uncertainty Components of SIAR**

| Parameter | Value | Absolute uncertainty |
|---|---|---|
| $D_1$ /Lsb | 12173 | 1.5 |
| $D_2$ /Lsb | 12151 | 1.5 |
| $D_S$ /Lsb | 32767 | 1.5 |
| $V_S$ /V | 5.1287 | 0.0001 |
| $R$ /Ω | 852.89 | 0.02 |
| $\Delta$ /Lsb | 10 | 3 |
| $S$ /mW/Lsb | $7.014\times10^{-3}$ | $4.7\times10^{-5}$ |
| $P_O$ /mW | 44.98 | 0.028 |

## 5. Conclusion

The fourth generation of SIAR is improved in both electrical and mechanical design, and adopts the measurement method of dynamic forecast compensated electrical power. There is a temperature pulse in the initial phase of radiant observation or electrical calibration. The temperature pulse increases the time of recovering equilibrium state. Thus the SIAR with big thermal time constant cannot adopt the measurement period of 90 second, which is generally used in IPC.

In this paper, the double exponential model of cavity temperature response is established. Simulation result illustrates that double exponential model is more accurate in practical measurement. A new characteristic parameter, named as non-equivalent response time, is proposed and experimentally measured. Experimental result illustrates that the non-equivalent response time is the origin of temperature pulse, and corresponds to a delay value of cavity temperature response curves. The temperature pulse is corrected by the method of inserting a delay time in measurement process. The insertion of delay time can compensate the non-equivalent response time. The time of recovering equilibrium state is shortened. The cavity temperature response model is simplified into a single exponential form. The accuracy of equilibrium temperature forecast is improved. Therefore, SIAR with large thermal time constant can adopt shorter measurement period, meanwhile measurement precision is 0.07%. Thus, The investigation of non-equivalent response time is important for the radiant calibration of SIAR. This correction method can also be used to optimize TSIMs for on-orbit measurement.

## Funding

This work is supported by the National Natural Science Foundation of China (NSFC) (NO.41227003 and NO. 41474161).

## References

[1] R. C. Willson, “Active cavity radiometer”, Appl. Opt, vol. 12, **(1973)**, pp. 810–817.
[2] R. C. Willson, “Active cavity radiometer type IV”, Appl. Opt, vol. 18, **(1979)**, pp. 179–188.
[3] R. E. Eplee Jr., K. R. Turpie, G. Meister, F. S. Patt, B. A. Franz and S. W. Bailey, “On-orbit calibration of the Suomi National Polar-Orbiting Partnership Visible Infrared Imaging Radiometer Suite for ocean color applications”, Appl. Opt, vol. 54, no. 8, **(2015)**, pp. 1984-2006.
[4] U. Schlifkowitz, W. Finsterle and W. Schmutz, “Development of a phase-sensitive absolute radiometer

 

for space and ground-based use, Research Report", 17th ESA Symposium on European Rocket and Balloon Programmers and Related Research, Sandefjord, NORWAY: ESA, **(2005)**, pp. 467-469.
[5] S. Mekaoui, S. Dewitte, C. Conscience and A. Chevalier, "Total solar irradiance absolute level from DIARAD/SOVIM on the International Space Station", Advances in Space Research, vol. 45, **(2010)**, pp. 1393-1406.
[6] R. B. Lee III, B. R. Barkstrom and R. D. Cess, "Characteristics of the earth radiation budget experiment solar monitors", Appl. Opt, vol. 26, no. 15, **(1987)**, pp. 3090-3096.
[7] R. W. Brusa and C. Frohlich, "Absolute radiometers (PM06) and their experimental characterization, Appl. Opt, vol. 25, no. 22, **(1986)**, pp. 4173-4180.
[8] Z. Yang, W. Fang, Y. Luo and Z. Xia, "Experimental characterization and correction of non-equivalence of Solar Irradiance Absolute Radiometer", Chin. Opt. Lett., vol. 12, no. 10, **(2014)**, pp. 101-202.
[9] W. Fang, H. Wang, H. Li and Y. Wang, "Total Solar Irradiance Monitor for Chinese FY-3A and FY-3B Satellites-Instrument Design", Solar Physics, vol. 289, **(2014)**, pp. 4711-4726.
[10] H. Wang, H. Li, J. Qi and W. Fang, "Total Solar Irradiance Monitor for the FY-3B Satellite-Space Experiments and Primary Data Corrections", Solar Physics, vol. 290, **(2015)**, pp. 645-655.
[11] D. Yang, W. Fang, X. Ye and B. Song, "High precision sun-tracking of spaceborne solar irradiance monitor", Opt. Precision Eng., vol. 22, no. 9, **(2014)**, pp. 2483-2490.
[12] D. Yang, W. Fang, X. Ye and B. Song, "Program-controlled sun-tracking precision of spaceborne solar irradiance monitor", Opt. Precision Eng., vol. 23, no. 7, **(2015)**, pp. 1813-1821.
[13] V. I. Sapritskii and M. N. Pavlovich, "Absolute radiometer for reproducing the solar irradiance unit", Metrologia, vol. 26, **(1989)**, pp. 81-86.
[14] W. Fang, B. Yu, H. Yao, Z. Li, C. Gong and X. Jin, "Solar irradiance absolute radiometer and international comparison", Acta Optica Sinica, vol. 23, **(2003)**, pp. 112-116.
[15] B. Yu, H. Yao and W. Fang, "Rapid Measurement Method of Absolute Radiometer by Using Forecast Radiation in Electrically Heating Compensation", Acta Optica Sinica, vol. 25, no. 6, **(2005)**, pp. 786-790.
[16] H. Wang, H. Li and W. Fang, "Timing Parameter Optimization for Comparison Experiments of TSIM", Appl. Opt., vol. 53, no. 9, **(2014)**, pp. 1719-1726.
[17] Y. Wang, W. Fang, C. Gong and B. Yu, "Dual cavity inter-compensating absolute radiometer", Opt. Precision Eng., vol. 15, no. 11, **(2007)**, pp. 1662-1667.
[18] S. Zhi, Y. Luo and J. Zhang, "The optimization design of a formula racing vehicle's front suspension system based on ADAMS", Journal of Harbin University of Science and Technology, vol. 20, no. 1, **(2015)**, pp. 80-84.
[19] J. Xu, X. Su and J. Feng, "Testing radiant thermal flux of flooring materials based on spline curve fitting", Journal of Harbin University of Science and Technology, vol. 19, no. 2, **(2014)**, pp. 125-128.
[20] Q. Fang, W. Fang and Y. Wang, "New shape of blackbody cavity: conical generatrix with an inclined bottom", Opt. Eng., vol. 51, no. 8, **(2012)**.

 